



INVESTIGATION THE EFFECT OF SIZE AND WEIGHT ON DRAG COEFFICIENT FOR FREE FALLING OF BALLS

Hassanain Ghani Hameed

Najaf Technical College/Automobile Department

Received:18/4/2009 ;Accepted :16/6/2010)

Abstract

The research aims to determine the drag coefficient for the free falling bodies with different size and weight using Infra Red transmitter and receiver circuits. The effects of size and weight on free falling bodies were studied. Carbon steel spheres with diameter of (0.8 – 8)mm and glass spheres with diameter of (0.5 – 17)mm, with different densities, were considered.

The relation between velocity and displacement was obtained from the experimental results, the drag coefficient was calculated after the establishment of the terminal velocity for free falling bodies. The relation between drag coefficients and Reynolds number were determined and compared with results of previous work.

Key Words : Drag Coefficient, Free Falling Balls, IR transmitter

الخلاصة

يهدف البحث إلى إيجاد معامل الإعاقة للأجسام حرة الحركة مختلفة الوزن والحجم باستخدام دائرتي الناقل والمستقبل للأشعة تحت الحمراء. تمت دراسة تأثير الأبعاد و الوزن في حركة الجسم الساقط، حيث أخذت كرات ذات كثافات مختلفة مصنوعة من الصلب الكربوني بأبعاد (٨ - ٠,٨) ملم وأخرى زجاجية بأبعاد (١٧ - ٠,٥) ملم. تم الحصول على علاقة تغير السرعة بالنسبة للإزاحة من النتائج العملية، حيث تم حساب معامل الإعاقة بعد الحصول على السرعة الثابتة من الجزء العملي للأجسام حرة السقوط، وعن طريق ذلك تم الحصول على علاقات معينة ما بين رقم رينولد و معامل الإعاقة. كانت النتائج التي تم الحصول عليها من الجانب العملي بالنسبة لمعامل الإعاقة مقاربة جدا للنتائج التي تم الحصول عليها من الأعمال السابقة.

Nomenclature

Symbol	Definition	Units
A_s	Surface area	m^2
C_D	Drag Coefficient	
F_b	Bouncy force	N
F_d	Drag force	N
V	volume	m^3
d	Diameter of the falling body	m
m	Mass of the falling body	Kg
m_{fluid}	Mass of the fluid	Kg
t	time	sec
v	velocity	m/s

1. Introduction

Understanding the motion of particles falling in viscous fluids is not only of fundamental theoretical interest, but it is also of importance in many practical applications and industrial processes such as falling-ball viscometry, transport of slurries, sedimentation, fluidization, etc, [P. Doleček et al., 2004].

For a relative motion between a body and a fluid, when a body moves through a fluid at rest, there are certain forces exerted on the body. The component of the force in the opposite direction of the relative motion is called drag force. Measuring this force has a variety of practical applications in the field of fluid mechanics for both internal and external flow. Different applications for external flow are the flow around aerofoil, flow around cylinders, wires, sedimentation, or improvement of combustion and the minimization of erosion by droplets in large turbines. This drag force was found to depend on several factors including, the shape, altitude, size of the body, the density and viscosity of the fluid. Also it depends on the velocity of the relative motion between the body and the fluid. Also the drag force depends on surface roughness of the body and the unsteadiness or turbulence in the fluid stream, [K.L. Kumar, 1997].

The drag force, at low velocities exerted between a solid body and a fluid flowing round it is due mainly to be pressure drag and the skin friction drag forces, [N. Mordant and J.F. pinton, 2000]. As for the latter part is caused by the viscous shear forces in the boundary layers forming on the surfaces of the body. On the other hand, pressure drag is caused by the eddies forming in the wake of the body, which cause eventually lower surface pressure and therefore resulting in drag

forces. In Bluff bodies the major part of the drag is the pressure drag. This creates interest in the investigation of the wake dynamics as the source of the pressure drag. The wake dynamics is reported to depend highly on the Reynolds number.

2. Theoretical Method

When a body is allowed to drop in a fluid, four forces act on the body: a gravitational force (F_{grv}), buoyancy (F_{buoy}), history force (F_h), and drag (F_d):

$$F_{net} = F_{grv} + F_{buoy} + F_h + F_d \quad (1)$$

The gravitational force (F_{grv}) will not change in magnitude as the object falls unless there is a change in the mass of the object:

$$F_{grv} = -m g \quad (2)$$

Where;

m: is the mass of the object

g: is the acceleration of gravity

Buoyancy (F_{buoy}) acts upwards, is equivalent in magnitude to the weight of the fluids displaced by the object, and not change in magnitude while the object falls

$$F_{buoy} = V_{body} \rho_{fluid} g \quad (3)$$

Where;

V_{body} : is the volume of the body.

ρ_{fluid} : is the density of the fluid.

History forces when a body immersed in a stationary fluid is suddenly set in motion, a flow field are induced in fluid. The kinetic energy associated with the fluid generated by moving the body against a drag force, [Chven – Yenchow, 1979]. This force is:

$$F_h = -\frac{1}{2} m_{fluid} \frac{dv}{dt} \quad (4)$$

Drag (F_d) acts upwards (for the body falling downward) and will increase in magnitude as

the velocity of the falling body increases that mean increase of Reynolds number.

$$F_d = \frac{1}{2} \rho_{fluid} v^2 A_s C_D \quad (5)$$

3. Governing Equations

Applying the Newton's law of motion to a spherical body, moving at subsonic speeds the wave drag can be safely omitted, [Xi, G.N., Hagiwara. Y. And Suzuki, K., 1995] has the form:

$$\frac{dv}{dt} = \frac{1}{A[B - C v^2 C_D]} \quad (6)$$

$$A = 1 + \frac{1}{2}(\rho_{\text{fluid}} / \rho_{\text{body}}) \quad (7)$$

$$B = [1 - (\rho_{\text{fluid}} / \rho_{\text{body}})]g \quad (8)$$

$$C = \frac{3(\rho_{\text{fluid}} / \rho_{\text{body}})}{4d} \quad (9)$$

For free falling the body will no longer accelerate but will continue to fall at the terminal velocity (v_t) which obtained by solving eq.(6) using a fourth order Runge – Kutta in time, as follows:

$$v_{n+1} = v_n + h/6 [K_1 + 2K_2 + 2K_3 + K_4] \quad (10)$$

$$K_1 = f(t_n) \quad (11)$$

$$K_2 = f(t_n + (h/2), v_n + (h/2)K_1) \quad (12)$$

$$K_3 = f(t_n + (h/2), v_n + (h/2)K_2) \quad (13)$$

$$K_4 = f(t_{n+1}, v_n + h K_3) \quad (14)$$

Where;

f : the function of velocity with respect to the time.

h : the time increment.

n : the counter.

The above equations are corporated in computer program to obtain the velocity of the falling body during different time intervals. Thus, the velocity of the free falling body with no acceleration (v_t) is:

$$v_t = \left[\frac{2 m g (\rho_{\text{body}} - \rho_{\text{fluid}})}{A_s \rho_{\text{body}} \rho_{\text{fluid}} C_D} \right]^{1/2} \quad (15)$$

May obtain the drag coefficient of the falling body from the above equation as follows:

$$C_D = \frac{2 m g (\rho_{\text{body}} - \rho_{\text{fluid}})}{A_s \rho_{\text{body}} \rho_{\text{fluid}} (v_t)^2} \quad (16)$$

4. Experimental Method

The aim of the experiments is to calculate the drag coefficient of a solid body (spheres) falling vertically under gravity and made from different material (carbon steel and glass with different density for the two materials) by measuring the velocity at different stage in the tube.

Basically, dividing the distance between two consecutive Infra Red (IR) Transmitters – Receiver couples by the time needed to cross it may obtain the body velocity.

4.1. Experimental rig

The experiment is performing in a glass tube (13cm x 13cm) and 200cm length. The end of the glass tube was filled by soil with height of 15cm to prevent the fracture of glass tube base by the falling body. The other part of tube was filled by water. Spheres made of steel and glass with different densities were used as falling body in the glass tube. Their specifications and main characteristics of motion are reported in **Table 1**. A pictorial view of the test rig is shown in **Fig.1**.

4.2. The Velocity Measuring Unit

Some researches [V. C. Kelessidis, 2003, P. Doleček et al., 2004, J. P. Owen and W. S. Ryu, 2005 and M. Garg et al., 2007] used more than one method to determine the velocity of the falling body after obtained the time interval travelling of the falling body between two specified points on the rig, such as using the stopwatch, high efficiency camera or electronic circuits.

In this work, the basic criterion of the velocity – measuring unit is to measure the time interval that takes the body to cross a pre – determined distance.

Evidently, the unit consists of many identical measurement groups; each group is integrated from the following elements:

1. IR Transmitter circuit and IR Receiver circuit

The Infra Red (IR) Transmitter sends out Infra Red rays, the IR Receivers sensed these rays. When the moving body passes by the IR Transmitter and the opening Receiver rays are cut. Consequently, the IR Receiver circuit gives a signal to the counter circuit to start counting the time elapsed before the body reaches the next IR Transmitter-Receiver couple positional at a predetermined distance. **Fig.2** shows the IR Transmitter circuit while **Fig.3** shows the IR Receiver circuit.

2. Signal processing circuit, the electronic circuit used for processing the electrical signal that is generated as the body cuts off the rays between the line of IR Transmitter and the opposing IR receiver as it passes through them. The electrical “pulse” of the first line sensor and receiver is

filtered and amplified through a flip-flop integrated circuit to trigger on the time counting circuit. The second “pulse” is generated as the body passes through the second line of IR Transmitter and IR Receiver. This “pulse” is manipulated in the same way, and it is used subsequently to stop the time counter.

3. Electrical Digital Clock Circuit a (1 MHz) crystal quartz oscillator generates a series of equally timed pulses; these pulses are further fed to a Dual Inline Package (DIP) switch speed selector, through a series of digital gates, in order to obtain a wide range of frequencies ranging from 500 Hz to 16 kHz according to the desired accuracy.

4. Electronic Time Counter / Display Circuit, kept fed by the electronic clock pulses, the output signal of the signal processing stage that result as the body passes through the first line of IR Transmitter and IR Receiver starts the counting.

Subsequently, the second signal that results as the body reaches the second line of the IR Transmitter and IR Receiver stops counting. The same sequence of events is repeated as the body passes through the following IR Transmitter-Receiver couples. Finally, the elapsed time between each two consequent events is displayed on the seven-segment screen.

Table (1): Results of Experimental Work for Solid Spheres.

Diameters of the spheres d (mm)	Types of material of spheres	Density of the spheres ρ_{body} (kg/m ³)	terminal velocity v_t (m/sec)	Reynolds number (Re)	Measured Drag coefficients of Spheres C_D
0.5	glass	2561	0.071	41.3	2.020
1.5	glass	2567	0.217	378.4	0.653
2	glass	2480	0.260	604.7	0.568
17	glass	2041	0.757	14964	0.404
0.8	Steel	7700	0.316	294	0.702
1	Steel	7851	0.383	445.3	0.611
2	Steel	8094	0.635	1476.7	0.458
3	Steel	8152	0.796	2776.7	0.443
4	Steel	8203	0.931	4330	0.435
6	Steel	8000	1.140	7953.5	0.422
8	Steel	7834	1.320	12279	0.410

5. Results

The measured terminal velocities are given in **Table 1**. In this case the motion has reached a stationary state, so that the terminal velocity is well defined. All the measurements present the mean value of the velocity obtained after averaging three readings of time. The drag coefficient was calculated by substitution in eq.(16).

Figure (4) shows the empirical curve of drag coefficients C_d versus Reynolds number (Re) from [J.B. Franzini and E.J. Finnemore, 1997], and the experimental obtained data for Reynolds number ranging from (40 to 15000). The experimental results show good agreement with [J.B. Franzini and E.J. Finnemore, 1997].

The drag coefficient was the same in the case of a fixed sphere measuring in wind tunnel and in the case of a free falling body when the experimental results was compared with the standard empirical drag measurements.

It is generally admitted this should be true at low Reynolds number, where the numerical and analytical studies agree that the drag is indeed given by the Stokes expression. However, at higher Reynolds number this result is not obvious. Indeed, it may be surprising that the particle reaches a stationary terminal velocity, and thus probably stationary momentums flux across the wake. This is an important difference with observations of the wake past a fixed body where the incoming flow is set at a constant uniform speed and the force acting on the body may take any value. In that case, instabilities in the wake were known to exist and were related to vortex shedding. In case of free falling, the constraint is just that the forcing gravity is constant; any change on the force felt by the sphere must be related to a change on the fluid motion.

Figure (5) shows comparison between the experimental and theoretical results for the velocity of falling steel spheres in water with displacement where the theoretical result its approximately less than the experimental results, the difference for large sphere at the first stage may be due to the velocity measured its the average velocity, the difference was appear and for the small sphere when its reach the terminal velocity from the first stage no difference between the average velocity measured and the local because the velocity was always constant.

Figures (6) and (7) show the relation of velocity for falling steel and glass spheres in water of properties from [L.W.Zhang et al., 1997] with time. The diameters of the steel spheres were (0.0008, 0.001, 0.002 and 0.003)m, while the diameters of the glass spheres were (0.0015, 0.002 and 0.017)m. The falling spheres velocity increases from zero until it reaches the terminal velocity, which is seen to increase with the diameter of the spheres. For smaller sphere, the Reynolds number

is relatively low and the boundary layer always remains laminar before the point of separation. Therefore, all the curves of the above Figures for falling spheres show the same trends.

Figure (8) shows comparison between the experimental and theoretical results for the velocity of falling glass spheres in water with displacement, where the theoretical result it's approximately less than the experimental results for the sphere diameter of 0.002 m. The behavior of the glass spheres is the same for the steel spheres in water, for the same diameter, with one difference is the terminal velocity value which increase with the spheres weight increasing. The maximum difference between the theoretical and experimental results is 3.11% for glass spheres which appear at 0.017m diameter, while for steel spheres is 1.85% at 0.008m diameter.

6. Conclusions

From the results of the current research, the following notations can be stated on the operation of the experimental system and the parameters affecting the motion of the spheres falling in water.

1. The measurements of velocity were average velocity in all cases, but when the body reaches the terminal velocity the local velocity become equal to average velocity.
2. The terminal velocity was obtained from experimental was very close to the terminal velocity was obtained in theoretical model.
3. The terminal velocity value depends on the weight of the falling body, for the same size, and it increase with the falling body weight increasing.
4. The consumptive time to reaches the terminal velocity depends on the falling body weight, which increases with the weight increasing.
5. The determination of drag coefficient from the measured terminal velocity was very close to the theoretical drag coefficient in these give the surety to the system.

7. References

- Chven - Yenchow "An introduction to computational fluid Mechanics" John wiley and sons, Inc. 1979.
- J.B. Franzini and E.J. Finnemore "Fluid mechanics" Ninth Edition, McGraw-Hill Company, 1997.
- J. P. Owen and W. S. Ryu " The effects of linear and quadratic drag on falling spheres", Eur. J. Phys. 26 (2005) 1085–1091

K.L. Kumar "Engineering fluid mechanics" Evrasia publishing house (p) LTD, 1997.

L.W. Zhang , D.K. Tafti, F.M. Najjar and S. Balachander "computations of flow and heat transfer in parallel – plate fin heat exchanges on the CM-5: effect of flow unsteadiness and three – dimensionally", Int. J. Heat transfer, vol. 40, pp. 1324 – 41, 1997.

M. Garg, P. Arun and F. M. S. Lima " Accurate measurement of the position and velocity of a falling object", Am. J. Phys. **75** (3), March 2007.

N.Mordant and J.F. pinton "velocity measurement of a setting sphere" The European physical journal B – 2000.

P. Doleček, H. Bendova, B. Šiška, and I. Machač "Fall of Spherical Particles through a Carreau Fluid", 31st International Conference of the Slovak Society of Chemical Engineering, Tatranske Matliare, Pap. 58(6) (2004) 397 – 403.

V. C. Kelessidis " Terminal Velocity of Solid Spheres Falling in Newtonian and non Newtonian Liquids", Tech. Chron. Sci. J. TCG, V, No 1-2, 2003.

Xi, G.N., Hagiwara. Y. And Suzuki, K., "Flow instability and augmented heat transfer of fin arrays", J. Enhanced heat transfer, vol. 2, pp. 87 – 32, 1995.



Fig. (1): Pictorial view of the test rig.

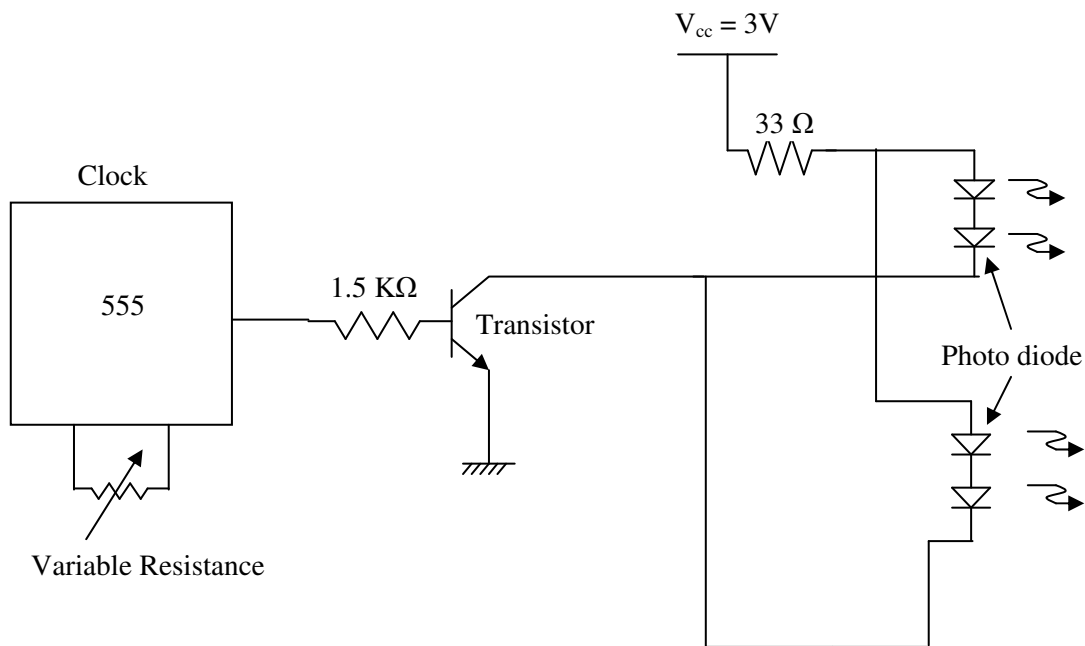


Fig. (2): IR transmitter Circuit

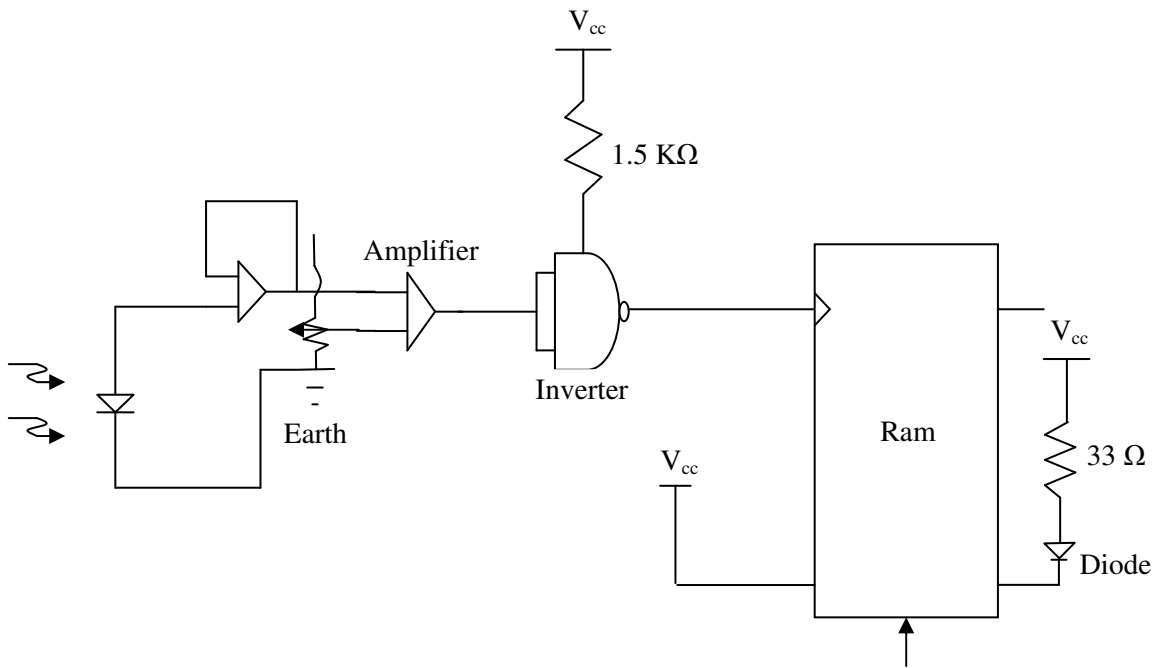


Fig. (3): IR Receiver circuit

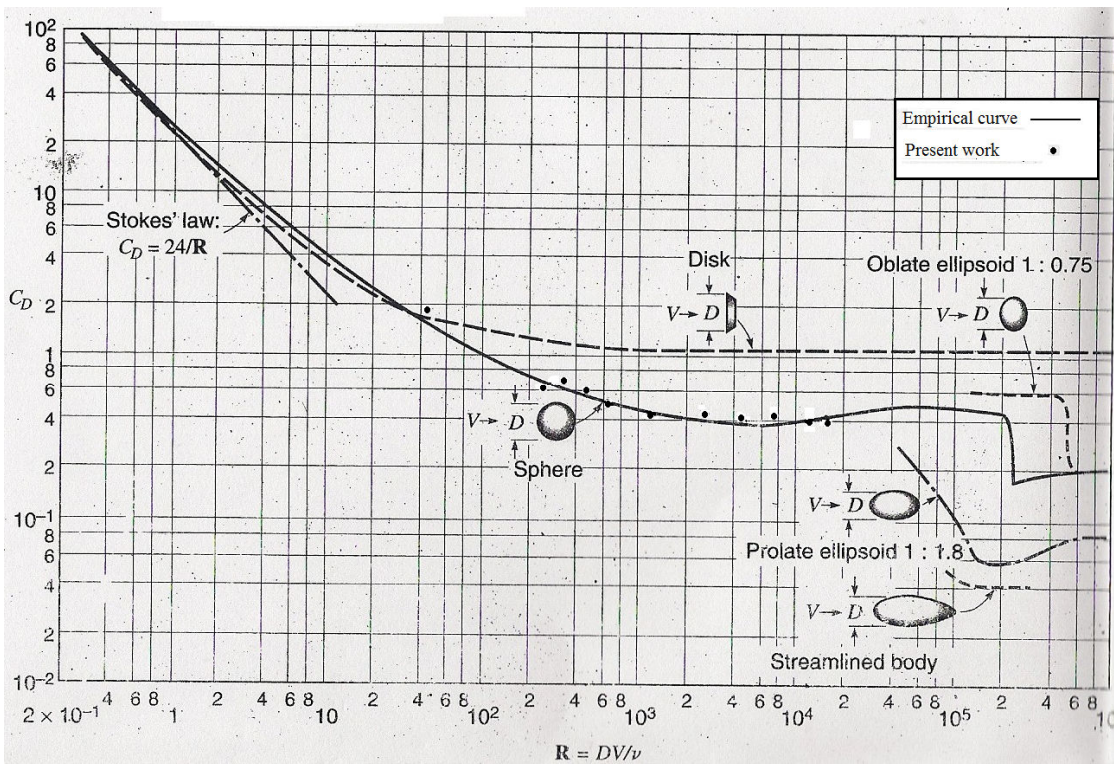


Fig. (4): Empirical curve for solids from [J.B. Franzini and E.J. Finnemore, 1997] for drag coefficient versus Reynolds number, and the experimental results for spheres.

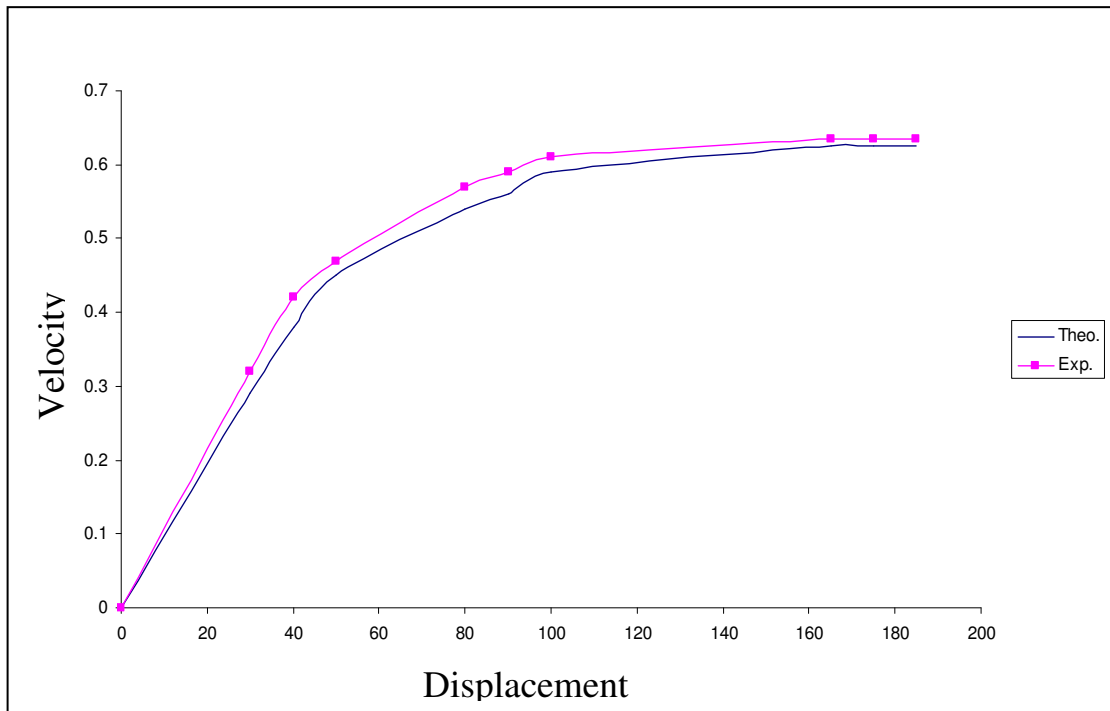


Fig. (5): Experimental and theoretical velocity change with displacement for falling steel sphere in water with diameter of 0.002 m.

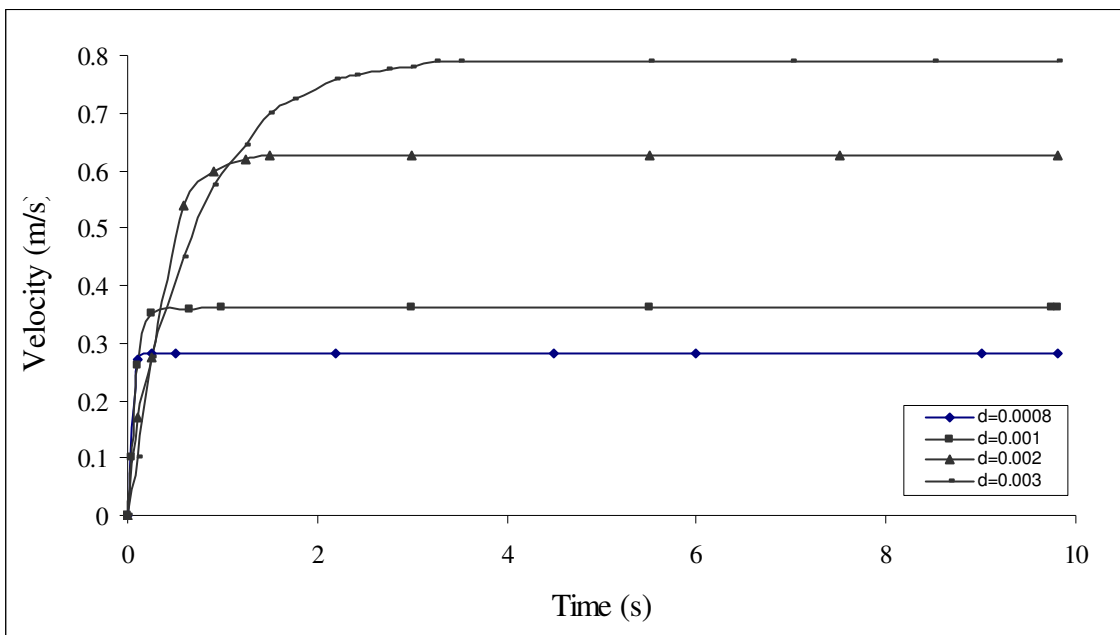


Fig. (6): Velocity change with time for different diameter of steel spheres falling in water.

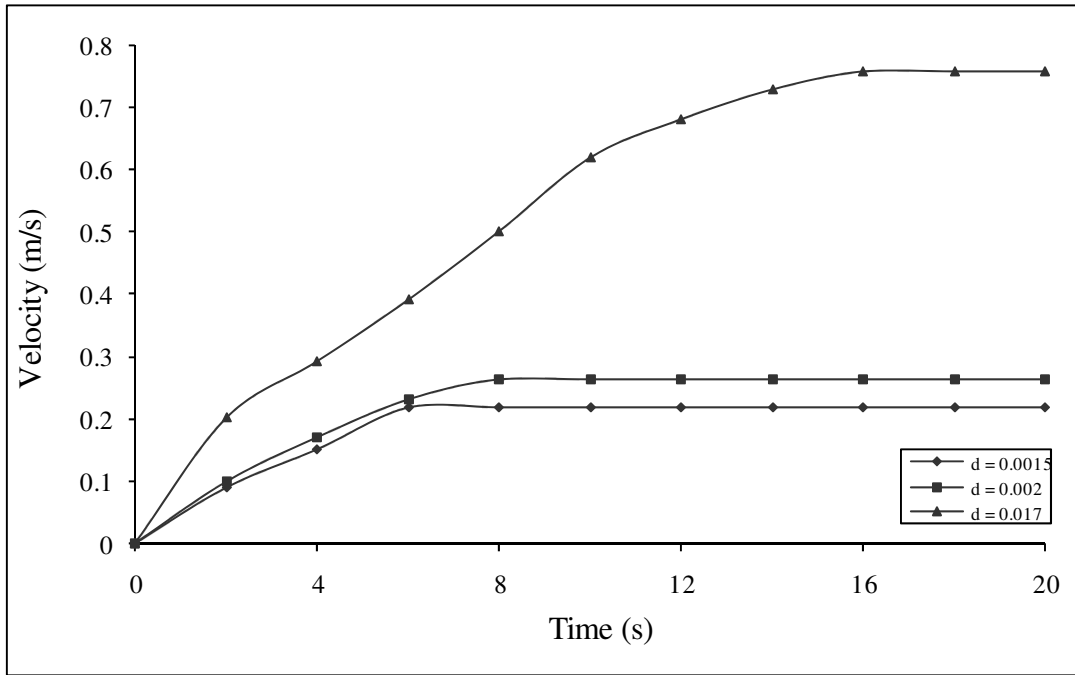


Fig. (7): Velocity change with time for different diameter of glass spheres falling in water.

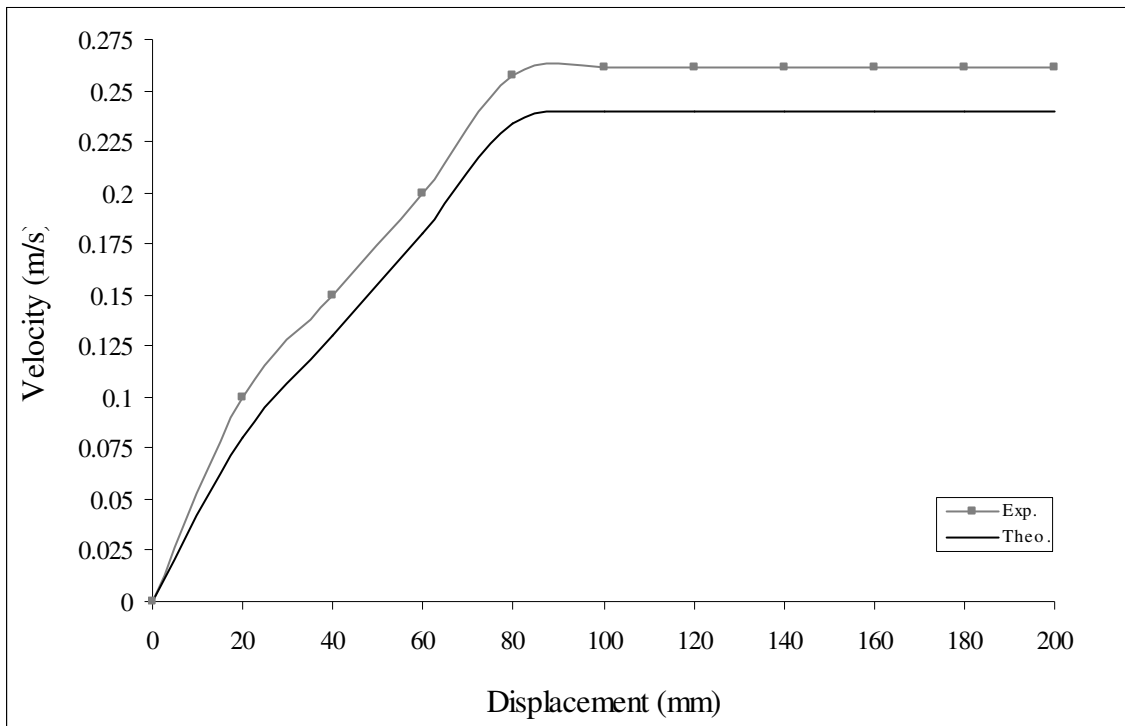


Fig. (8): Experimental and theoretical velocity change with displacement for falling glass sphere in water with diameter of 0.002 m.